The Egyptian Journal of Radiology and Nuclear Medicine (2014) **45**, 35–47

Egyptian Society of Radiology and Nuclear Medicine

The Egyptian Journal of Radiology and Nuclear Medicine

www.elsevier.com/locate/ejrnm
www.sciencedirect.com

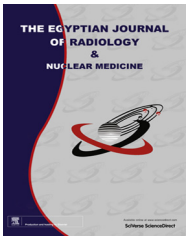

ORIGINAL ARTICLE

Role of magnetic resonance imaging in pre-operative assessment of ano-rectal fistula

Rania E. Mohamed *, Dina M. Abo-Sheisha

Radiodiagnosis Department, College of Medicine, Tanta University, Egypt

Received 1 September 2013; accepted 28 October 2013
Available online 28 November 2013

KEYWORDS

Magnetic resonance imaging;
Ano-rectal;
Fistula

Abstract *Aim of the work:* To evaluate the role of magnetic resonance imaging (MRI) in preoperative assessment of ano-rectal fistula and tracing its full extent and relationship.
Materials and methods: Twenty-four patients with ano-rectal fistula were enrolled in this study. They were examined with different MRI sequences for evaluation of the fistulas and their extent. Fistulas were classified according to St. James's University Hospital MRI based classification system (which correlates the Parks surgical classification to anatomic MRI findings) into 5 grades. Then, interrelation between surgical and MRI findings was statistically analyzed with evaluation of the accuracy of each MRI sequence used.
Results: Grade 1 was the most frequent (37.5%) type of ano-rectal fistula. The most common location of the internal opening of the fistula was at 6 o'clock position. Combination of oblique coronal and axial planes of contrast-enhanced fat suppressed T1-weighed fast spin-echo (CE FS T1WFSE) sequence images showed the highest accuracy (99.4%) in diagnosis of ano-rectal fistula.
Conclusion: MRI is a useful imaging tool in the preoperative assessment of ano-rectal fistula. A significant accordance between surgical and MRI findings was achieved by using combination of coronal and axial planes of CE FS T1WFSE sequence images.

1. Introduction

Ano-rectal fistulas are chronic inflammations of perianal tissues with a connection between the skin of the perineum and the anal canal (1). An understanding of ano-rectal anatomy is necessary to perfectly classify fistulas before choosing an appropriate surgical therapy (2). The anal canal consists of two muscular cylinders. The inner cylinder, called the internal anal sphincter, is a 3-cm long thickened continuation of the circular smooth muscle of the rectum and extends from the ano-rectal junction to 1–1.5 cm below the dentate line. The outer cylinder, called the external anal sphincter, is a 4-cm long

Abbreviations: FS T1WFSE, fat suppressed T1-weighted fast spin-echo; FS T2WFSE, fat suppressed T2-weighted fast spin-echo; CE FS T1WFSE, contrast enhanced fat suppressed T1-weighted fast spin-echo

* Corresponding author. Tel.: +20 1003201025.
E-mail addresses: Rany1997@yahoo.com (R.E. Mohamed), dinamogh@hotmail.com (D.M. Abo-Sheisha).

Peer review under responsibility of Egyptian Society of Radiology and Nuclear Medicine.

ELSEVIER Production and hosting by Elsevier

0378-603X © 2014 Production and hosting by Elsevier B.V. on behalf of Egyptian Society of Radiology and Nuclear Medicine.
Open access under CC BY-NC-ND license. http://dx.doi.org/10.1016/j.ejrnm.2013.10.008

Table 1 Parameters of the used MR imaging sequences for ano-rectal fistulas.

MRI sequences	Non-contrast scans		Non contrast fat suppressed scans		Contrast-enhanced fat suppressed scans
	T1WFSE	T2WFSE	FS T1WFSE	FS T2WFSE	FS T1WFSE with magnivest
Imaging plane	Axial and coronal	Sagittal, axial and coronal	Axial and coronal	Sagittal, axial and coronal	Sagittal, axial and coronal
TR/TE (msec)	450/14	4500/110	560/14	4500/110	560/14
FOV (cm)	26 × 26	24 × 24	26 × 26	24 × 24	26 × 26
Section thickness (mm)	4.0	4.0	4.0	4.0	4.0
Intersection gap (mm)	0.8	0.8	0.8	0.8	0.8
Matrix	384 × 224	320 × 256	384 × 224	320 × 256	384 × 224

T1WFSE: T1-weighted fast spin-echo, T2WFSE: T2-weighted fast spin-echo, FS T1WFSE: fat suppressed T1W fast spin-echo, TR/TE: repetition time/echo time, FOV: field of view, T1W: T1-weighted, T2W: T2-weighted, FSE: fast spin-echo, FS: fat suppressed.

downward extension of the puborectalis muscle (3). The inter-sphincteric plane lies between these two cylinders. The pectinate or dentate line, which is located in the middle portion of the internal anal sphincter, separates the transitional and columnar epithelium of the rectum from the squamous epithelium of the anus. The anal crypts are present at this dentate line. Anal glands exist at the base of many of these crypts and occasionally penetrate into the inter-sphincteric space (4).

The perianal fistulas are thought to be the result of anal gland obstruction, with secondary abscess formation and external rupture decompression through one of several fairly predictable routes. The internal origin of the fistula usually begins from the middle of the anal canal at the dentate line (3,5,6). Because recurrence is one of the most important problems following surgery, identification of the extensions of the ano-rectal fistula with proper imaging methods decreases the percentage of its recurrence (7).

The magnetic resonance imaging (MRI) plays an important role in the preoperative evaluation of the ano-rectal fistulas as it allows identification of the infected tracts and abscesses as well as detailed anatomic descriptions of the relationship between the fistula and the anal sphincter complex (6,8).

There are two main classification systems for ano-rectal fistula; the classification proposed by Parks et al. in 1976 (9), which was created for surgical use, and the St. James University Hospital classification, which was developed based on an MRI examination (10,11).

The aim of this study was to evaluate the role of MRI in preoperative assessment of ano-rectal fistula with tracing its full extent and relationship to the sphincter complex by using different MRI sequences.

2. Materials and methods

This study was carried out in the period from May 2011 to November 2012 in the Radiology department of our institution. Study participants were 24 patients (16 males and 8 females) with initial clinical diagnosis of ano-rectal fistula. All patients were presented with local pain and discharge, in addition to associated abscess in 5 of them. They were evaluated by pelvic MRI 3–24 days before being subjected to surgery. Patients were excluded from the study when they had a history of autoimmune disease, diabetes mellitus or recurrent perianal fistula. An official permission to carry out the study was obtained from the local medical research ethics committee. Patient consent to participate in the study was obtained.

The MRI sequence images were performed by using 1.5-Tesla unit system (*Signa Horizon SR 120*; *General Electric Medical Systems*, *Milwaukee*, *WI*, *USA*) with a phased-array coil. The patients were placed in the supine position and a phased-array coil was used for image acquisition. The imaging volume was planned to incorporate the distal rectum and subcutaneous tissue with inclusion of the anal canal, the sphincter muscles, the ischio-rectal fossa, the levator muscle and the supralevator space.

The following MRI protocol was done for all patients: non contrast scans; including oblique axial and coronal T1-weighted fast spin-echo (T1WFSE) and T2-weighted fast spin-echo (T2WFSE), non contrast with fat suppression scans; including oblique axial fat suppressed T1WFSE (FS T1WFSE) and oblique axial and coronal as well as sagittal fat suppression T2WFSE (FS T2FSE), and contrast-enhanced MRI (CE-MRI) scans; including oblique axial and coronal as well as sagittal fat suppressed T1WFSE, which were obtained after intravenous automatic injection of 0.1 mmol/kg body weight of gadolinium based contrast agent; Magnevist [gadolinium diethylenetriamine pentaacetic acid (Gd-DTPA); Magnevist; Berlex, Montvale, NJ], using an automated power injector (Medrad; Warrendale, PA, USA) at a rate of 1 ml/s. The used MRI parameters are tabulated in Table 1 and the used protocol is shown in Fig. 1.

The target of MRI was to answer the decisive surgical questions previous to the surgical interference. So, the following items were assessed for each of the used MRI sequences: the type of the fistula, location of the internal opening, the presence or absence of sinus tracts, abscesses and a horseshoe component as well as coexisting inflammation. The type of the fistula was evaluated according to the St. James's University Hospital MRI classification system (8) which correlates Parks surgical classification (9) to anatomical MRI findings in the axial and coronal planes (Tables 2 and 3; Fig. 2). The location of the internal opening was identified on axial images using the "anal clock" with the 12 o'clock position located anterior and the 6 o'clock position located posterior (12) (Fig. 1C).

A fistula with a tract medial to the levator plate or puborectalis muscle is supralevator, while a fistula lateral to these muscles is infralevator. Complicated primary tracts with secondary tracts, extensions or abscesses were defined by their anatomical location: ischio-anal, intersphincteric, or supralevator and they were considered horseshoe if crossing the midline to the contra-lateral side (2). Fistulous tracts were differentiated from abscesses by using the criteria of Laniado

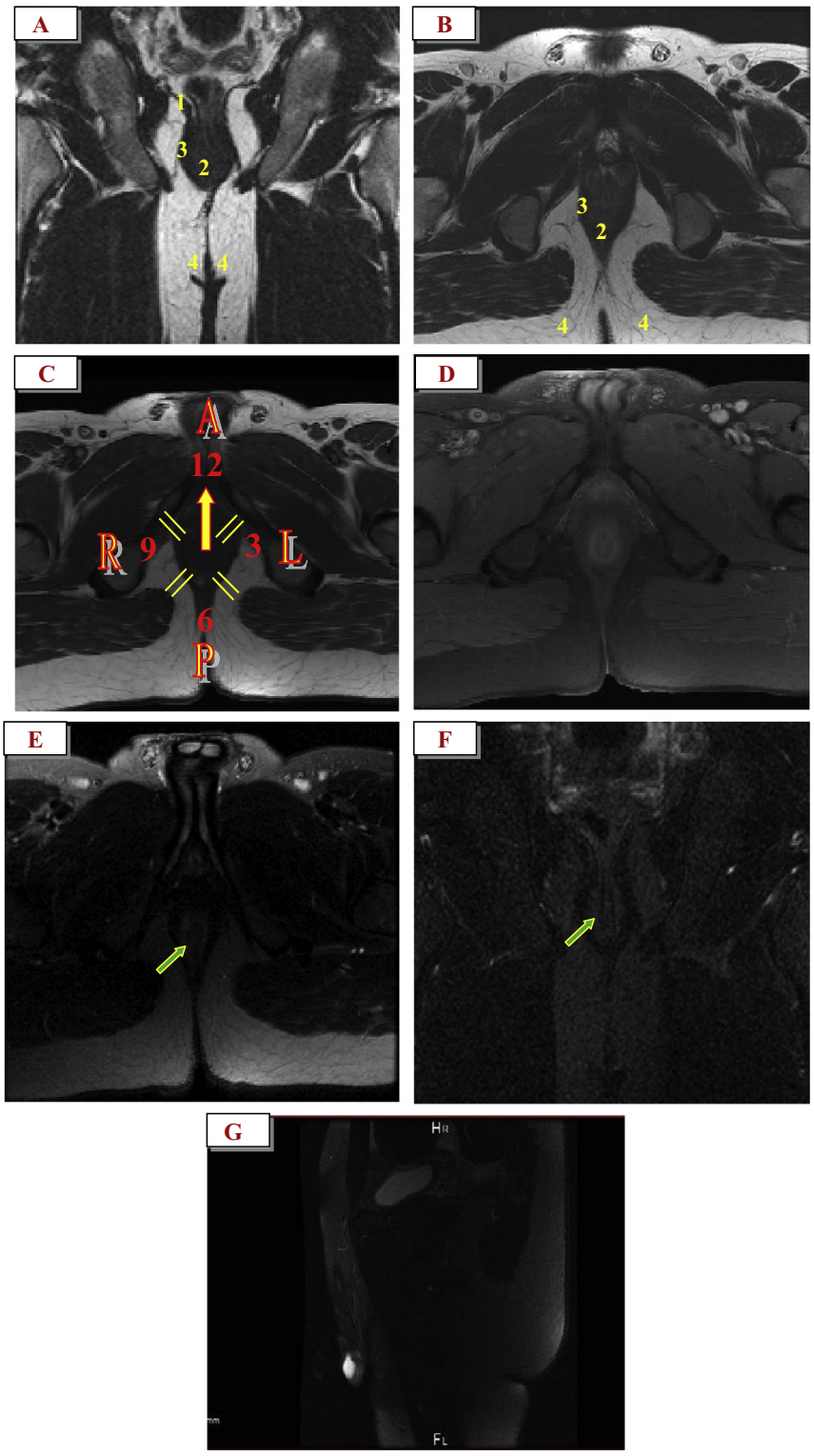

Fig. 1 (A, B, C, D, E, F and G) Illustrates the protocol used in our study in a normal male subject with unremarkable peri-anal area. Coronal (A) and Axial (B) planes of T2WFSE sequence images show normal peri-anal area, where (1) is the levator ani muscle, (2) is the internal sphincter, (3) is the external sphincter and (4) is the ischioanal fossa. Axial T1WFSE (C) sequence image shows the anal clock. The 12 o'clock position corresponds to the anterior (A) aspect of the midline or the perineum, the 3 o'clock corresponds to the left (L) lateral aspect, the 6 o'clock corresponds to the posterior (P) aspect of the midline or intergluteal cleft, and the 9 o'clock corresponds to the right (R) lateral aspect. Additionally, axial contrast-enhanced FS T1WFSE (D) image shows no evidence of fistulous tract or abscess. Furthermore, axial (E), coronal (F) and sagittal (G) FS T2WFSE images reveal normal intersphincteric space (green arrow) with no abnormal signal intensity.

Table 2 MRI grading of ano-rectal fistula (8) (Fig. 2A).

Grade	Description
1	Simple linear inter-sphinctric fistula
2	Inter-sphincteric fistula with inter-sphincteric abscess or secondary fistulous track
3	Trans-sphincteric fistula
4	Trans-sphincteric fistula with abscess or secondary track within the ischioanal or ischiorectal fossa
5	Supralevator and translevator disease

Table 3 Parks classification of ano-rectal fistula (9) (Fig. 2B).

Fistula type	Description
Inter-sphincteric	Confined to inter-sphincteric plane, does not cross external sphincter or levator muscles
Trans-sphincteric	Track passes radially through external sphincter
Supra-sphincteric	Track passes upward within inter-sphincteric plane over puborectalis muscles and descends through levator muscles to the ischiorectal fossa
Extra-sphincteric	Course is completely outside external sphincter

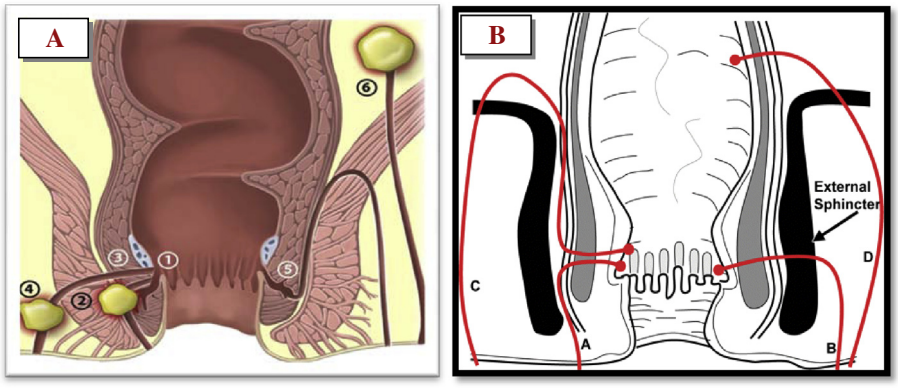

Fig. 2 (A and B): Coronal diagrams illustrate types of ano-rectal fistulas according to St. James classification (Fig. 2-A from 1 to 6), and Parks classification (Fig. 2-B from A to D); whereas: (1) points for grade 1 (simple intersphincteric), (2) points for grade 2 (intersphincteric with abscess, in which fistulas and abcesses are confined by external anal sphincter), (3) points for grade 3 (simple transsphincteric), (4) points for grade 4 (transsphincteric with abscess in which fistulas both involve ischiorectal or ischioanal fossae), (5 and 6) point for grade 5 (suprasphincteric fistulas and extrasphincteric fistulas), (Quoted from O'Malley, et al.) (10). Also, (A) points for intersphincteric fistula, (B) points for transsphincteric fistula, (C) points for suprasphincteric fistula and (D) points for extrasphincteric fistula, (Quoted from de Miquel Criado, et al.) (8).

et al. (13) in which fistulas were defined as being fluid–fluid tubular structures with a diameter smaller than 10 mm and abscesses were larger than 10 mm. Air pockets within the fluid collection also suggested the presence of abscess. MRI findings were then correlated with the surgical results.

2.1. Statistical analysis

The collected data were revised; coded, tabulated and analyzed using the statistical package for social sciences (SPSS) for windows version 18.0 software package (SPSS Inc., Chicago, IL). The obtained results were compared using the Chi-square and Fisher's exact tests for qualitative data. The accuracy of MRI with eight different sequences in the diagnosis of the peri-anal fistula (its sinus track, internal opening associated abscess, inflammatory changes, horseshoe and supralevator extensions) was statistically analyzed according to the final surgical results. $P < 0.05$ was considered statistically significant.

3. Results

Twenty-four patients with initial clinical diagnosis of ano-rectal fistula and/or abscess were included in this study. They were 16 males and 8 females with a ratio of 2:1. Their ages ranged from 23 to 67 years with a mean of 45.5 ± 22.5 years. According to the "anal clock" on MRI axial images, the internal openings of the ano-rectal fistulas were identified in all of our patients and their most common location was at 6 o'clock position as it was encountered in half of them, as shown in Table 4.

The MRI grading of ano-rectal fistula revealed that grade I was the commonest type as it was recognized in 9 patients

Table 4 Distribution of the different locations of the internal opening on MRI axial images in patients with ano-rectal fistula ($n = 24$).

Location of internal opening	Number (No.)	Percent (%)
At 6 o'clock	12	50
At 12 o'clock	6	25.0
At 7 o'clock	2	8.3
At 4 o'clock	2	8.3
At 5 o'clock	1	4.2
At 11 o'clock	1	4.2
Total	**24**	**100**

(37.5%). By MRI examination branching fistula was present in 5 (20.8%) patients (Table 5), but according to surgical data, branching fistula was present in 6 patients (Table 6). So, one patient with a faint high secondary fistulous tract was missed by MRI.

On estimating the average accuracies of the used MRI sequences in diagnosing the ano-rectal fistula, the present study revealed that the highest accuracy was reached through the contrast enhanced axial and coronal FS T1WFSE sequences (99.40%), while the lowest accuracy was present with the sagittal T2WFSE sequence (89.29%). Furthermore, we used Fisher's exact and Chi-square tests to signify the correlation between findings obtained by the used MRI sequences and surgical findings. The contrast-enhanced axial and coronal FS T1WFSE showed a highly significant correlation with the surgical findings ($P < 0.001$). Also, each of the axial and coronal T2WFSE as well as the axial and coronal FST2WFSE showed a significant correlation with the surgical findings ($P = 0.03$ for each), as shown in Table 6.

3.1. Cases

The figures from Figs. 3–10 demonstrate a sample of selected cases of our study, each figure outlines one case.

Fig. 3 demonstrates a patient with a right simple linear inter-sphincteric fistula (grade 1 ano-rectal fistula). Axial plane of T1WFSE (A), axial (B) and coronal (C) planes of T2WFSE, coronal planes of FS T2WFSE (D) and contrast-enhanced FS T1WFSE (E) sequence images show an ano-rectal fistula with a simple non branching tract which is seen within the right inter-sphincteric space (red arrows) with no secondary tract or any extensions beyond the external sphincter. Axial plane of FS T2WFSE (F) sequence image shows the site of the internal opening of the fistula at 7 o'clock position (the yellow arrow).

Fig. 4 demonstrates a patient with a right simple linear inter-sphincteric fistula (grade 1 ano-rectal fistula). Axial plane of contrast enhanced FS T1WFSE (A) sequence image shows an ano-rectal fistula with a simple non branching tract which is seen within the right inter-sphincteric space (white arrows at A image) with no secondary tract or any extension beyond the external sphincter. Axial plane of FS T2WFSE (B) sequence image shows the internal opening of the fistula at 12 o'clock position (the red arrow at B image) with faint enhancement of the minimal inflammatory changes around the fistulous tract and its internal opening. However, a clear demarcation between the external and internal anal sphincters is obviously seen.

Fig. 5 represents a patient with grade 2 left inter-sphincteric fistula with an abscess formation. Axial contrast enhanced FS T1WFSE (A) image shows diffuse circumferential inflammatory changes with homogenous enhancement more pronounced in the left side of the intersphincteric space. Coronal planes of T2WFSE (B) FS T2WFSE (C) sequence images demonstrate an ano-rectal fistula within the left intersphincteric space (yellow arrows) with obviously seen left intersphincteric abscess cavity (red arrows) inseparable from the primary non branching intersphincteric track. However, there is no secondary tract, horseshoe or supralevator extension.

Fig. 6 represents a patient with grade 3 right trans-sphincteric non branching fistula with no secondary tract, associated abscess, horseshoe or supralevator extensions. Non-contrast axial T1WFSE (A) and axial T2WFSE (B) as well as axial, coronal and sagittal FS T2WFSE (C, D and E, respectively) images show a right trans-sphincteric non branching fistula with the point of entry of the fistulous tract obviously seen in the midline posteriorly at the 6 o'clock position (red arrow at C image) and the tract itself is seen traversing the external sphincter to the ischio-rectal fossa (yellow arrows at A, B, C and D images).

Fig. 7 represents a patient with grade 4 right branching trans-sphincteric fistula with the secondary track seen within the ischiorectal fossa. Axial T1WFSE (A), axial (C) and coronal (D) T2WFSE, and coronal FS T2WFSE (E) images demonstrate a right sided branching fistulous tract with two branches: the primary, trans-sphincteric branch at a higher level on the right lateral wall of the anal canal near the levator plate (the red arrows at A, C, D and E) and the secondary lower branch is seen in the right inter-sphincteric space (the yellow arrows at A, C, D and E images). Axial plane of FS T2WFSE

Table 5 Distribution of MRI grades of ano-rectal fistula and its associated MRI findings in the studied patients ($n = 24$).

Ano-rectal fistula grading on MRI			Associated MRI findings				
			Fistulous tract		Horseshoe extension	Para-anal abscess	Supra-levator extension
Grade	No	%	Simple non branching	Branching			
Grade 1	9	37.5	9	0	0	0	0
Grade 2	3	12.5	2	1	1	1	0
Grade 3	3	12.5	3	0	0	0	0
Grade 4	5	20.8	3	2	1	2	1
Grade 5	4	16.7	2	2	2	2	4
Total	**24**	**100**	**19 (79.2%)**	**5 (20.8%)**	**4 (16.7%)**	**5 (20.8%)**	**5 (20.8%)**

Table 6 Accuracy of different MRI sequences in diagnosis of ano-rectal fistula and its associated findings in correlation to surgical data ($n = 24$).

Findings in ano-rectal fistula cases		The used MRI sequences and imaging planes							
		T1WFSE	T2WFSE		FS T1WFSE	FS T2WFSE		Contrast enhanced FS T1WFSE	
		Axial and coronal	Axial and coronal	Sagittal	Axial and coronal	Axial and coronal	Sagittal	Axial and coronal	Sagittal
Identified internal opening		83.33% (20/24)	91.67% (22/24)	83.33% (20/24)	87.50% (21/24)	91.67% (22/24)	87.50% (21/24)	100% (24/24)	91.67% (22/24)
Sinus tract	Simple non-branching	91.67% (16/18)	95.83% (17/18)	91.67% (16/18)	95.83% (17/18)	95.83% (17/18)	91.67% (16/18)	100% (18/18)	91.67% (16/18)
	Branching	87.50% (3/6)	91.67% (4/6)	87.50% (3/6)	91.67% (4/6)	91.67% (4/6)	87.50% (3/6)	95.83% (5/6)	91.67% (4/6)
Abscess		95.83% (4/5)	100% (5/5)	95.83% (4/5)	100% (5/5)	100% (5/5)	95.83% (4/5)	100% (5/5)	95.45% (4/5)
Horseshoe extension		95.83% (3/4)	95.83% (3/4)	91.67% (2/4)	95.83% (3/4)	95.83% (3/4)	91.67% (2/4)	100% (4/4)	95.45% (3/4)
Supralevator extension		95.83% (4/5)	100% (5/5)	95.83% (4/5)	100% (5/5)	100% (5/5)	95.83% (4/5)	100% (5/5)	95.45% (4/5)
Associated inflammatory changes		79.17% (19/24)	83.33% (20/24)	79.17% (19/24)	91.67% (22/24)	91.67% (22/24)	87.50% (21/24)	100% (24/24)	95.8% (23/24)
Accuracy (%)		89.88	94.04	89.29	94.64	95.83	91.07	99.40	94.31
X^2		0.375	5.042	0.375	3.375	5.042	0.386	18.375	1.042
P-value		0.54	0.03*	0.54	0.07	0.03*	0.43	< 0.001*	0.30

* Significant (P-value < 0.05).

(B) sequence image demonstrates the site of the internal opening of the two branches of the fistula at 6 o'clock position (the green arrows at B image). Coronal (F), axial (G and H) and sagittal (I) planes of contrast enhanced FS T1WFSE sequence images demonstrate the enhancement of both branches of the fistula with enhancement of the surrounding inflammatory reaction (the blue arrows).

Fig. 8 represents a patient with grade 4 right trans-sphincteric fistula with an abscess in the right ischioanal fossa. Axial FS T2WFSE (A and B) as well as axial contrast enhanced FS T1WFSE (C) images show a right trans-sphincteric fistula (yellow and red arrows on A and B images, respectively) with enhancement of the inflammatory reactions around the fistulous tract as well as enhancement of the associated abscess cavity which is seen inseparable from the fistulous tract in the right ischioanal fossa (light green arrow on C image). There are no secondary tract, horseshoe or supralevator extensions.

Fig. 9 demonstrates a patient with grade 4 trans-sphincteric fistula associated with a branching fistulous tract with an abscess formation in the ischioanal fossa and horseshoe extension in the posterior inter-sphincteric space. Axial T1WFSE (A), coronal contrast enhanced FS T1WFSE (B and C) and sagittal FS T2WFSE (D) sequence images show two fistulous tracts: the primary, trans-sphincteric branch on the left lateral wall of the anal canal, where an associated abscess (white arrows at C and D images) is seen with the signal void appearance of pus as well as a secondary inter-sphincteric tract at right side (yellow arrow at B image) with associated horseshoe extension in the posterior inter-sphincteric space (red arrows at A and B images).

Fig. 10 demonstrates a patient with grade 5 right supralevator (supra-sphincteric) fistula. Coronal T2WFSE (A) shows right sided high level supra-sphincteric fistulous tract which arise from anal canal before ascending to the supralevator space. The axial contrast enhanced FS T1FSE (B) shows the position of the internal opening of the fistula at 6 o'clock. There is no associated secondary tract or abscess formation.

4. Discussion

Ano-rectal fistulas comprise a heterogenic group of pathologies of the terminal part of the gastrointestinal tract and perineal area (14,15). Most of the fistulas are of glandular origin and to some extent straight, slightly elliptical tract starting in the peri-anal area, with the internal orifice in the anal canal. The main role in pathophysiology of fistula formation is played by the location and the number of perianal glands specific for that region, as well as the direction in which the infection spreads along anatomical planes (1,15,16).

Some fistulas recur because of distant sepsis resulting in incomplete treatment; this is chiefly the case if there is supralevator extension. Also, management problems take place if the primary track crosses the external sphincter high in the anal canal with high internal opening that is not suspected pre-operative by clinical examination alone with a risk of subsequent incontinence due to substantial sphincter division (16). Therefore, accurate preoperative assessment of the perianal fistulous tract is the main target of the preoperative investigations aiming to eliminate the infection while preserving anal continence as well as reduction of the incidence of recurrence with determination of the surgery efficiency (1,17).

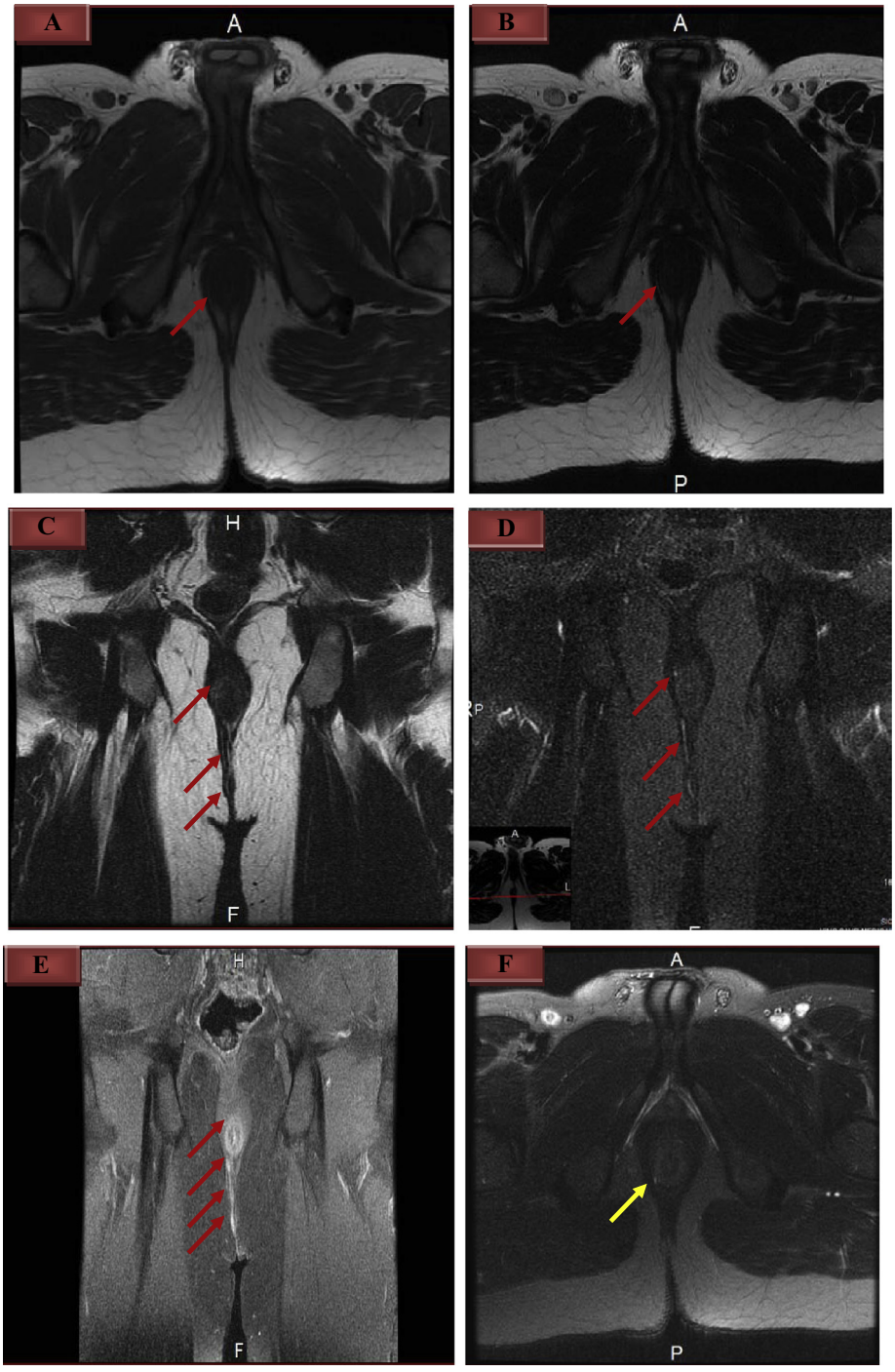

Fig. 3 (A, B, C, D, E and F) demonstrates a patient with a right simple linear inter-sphincteric fistula (grade 1 ano-rectal fistula). Axial plane of T1WFSE (A), axial (B) and coronal (C) planes of T2WFSE, coronal planes of FS T2WFSE (D) and contrast-enhanced FS T1WFSE (E) sequence images show an ano-rectal fistula with simple non branching tract which is seen within the right inter-sphincteric space (red arrows) with no secondary tract or any extensions beyond the external sphincter. Axial plane of FS T2WFSE (F) sequence image shows the site of the internal opening of the fistula at 7 o'clock position (the yellow arrow).

The MRI of ano-rectal fistula with the use of the superficial body coil is a rapid, well-tolerated technique which might play an important role in the preoperative evaluation of ano-rectal fistula and its management as well. It does not need any previous patient preparation and can accurately assess the surgical anatomy of the ano-rectal region (18).

The classification proposed by Parks et al. (9) was much criticized as it does not include the submucosal fistulas, very superficial and sphincteric structures. Since pertinent MR imaging findings are not included in the Parks classification, an MR imaging–based classification was proposed by Morris et al. (3) in a study with more than 300 patients at the St.

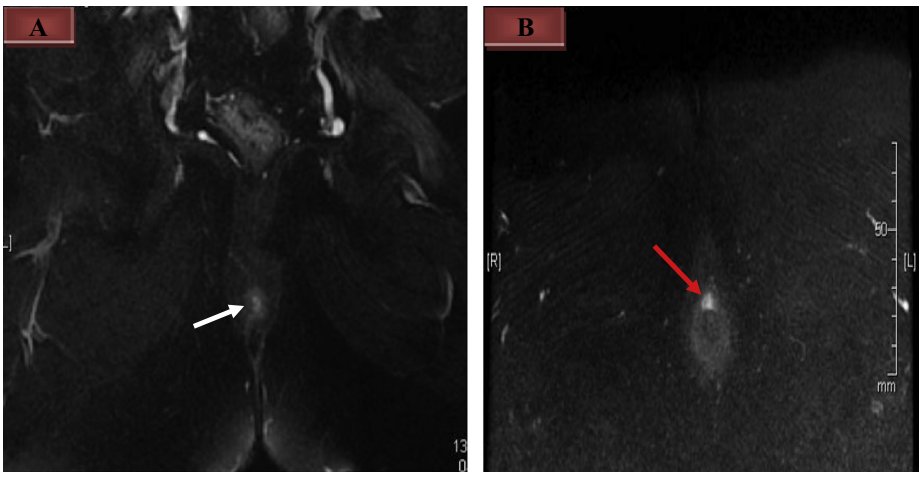

Fig. 4 (A and B) demonstrates a patient with a right simple linear inter-sphincteric fistula (grade 1 ano-rectal fistula). Axial plane of contrast enhanced FS T1WFSE (A) sequence image shows an ano-rectal fistula with simple non branching tract which is seen within the right inter-sphincteric space (white arrows at A image) with no secondary tract or any extension beyond the external sphincter. Axial plane of FS T2WFSE (B) sequence image shows the internal opening of the fistula at 12 o'clock position (the red arrow at B image) with a faint enhancement of the minimal inflammatory changes around the fistulous tract and its internal opening. However, a clear demarcation between the external and internal anal sphincters is obviously seen.

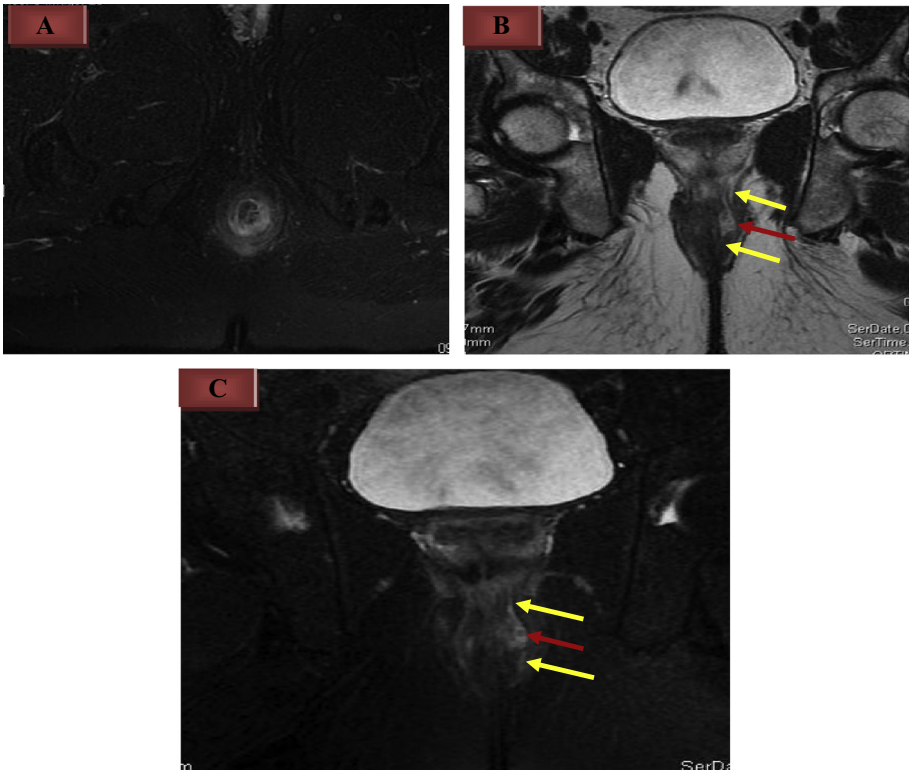

Fig. 5 (A, B and C) represents a patient with grade 2 left inter-sphincteric fistula with an abscess formation. Axial contrast enhanced FS T1WFSE (A) image shows diffuse circumferential inflammatory changes with homogenous enhancement more pronounced in the left side of the intersphincteric space. Coronal planes of T2WFSE (B) FS T2WFSE (C) sequence images demonstrate an ano-rectal fistula within the left inter-sphincteric space (yellow arrows) with obviously seen left intersphincteric abscess cavity (red arrows) inseparable from the primary non branching intersphincteric track. However, there is no secondary tract, horseshoe or supralevator extension.

James's University Hospital (Leeds, England), to relate the Parks surgical classification to anatomic MR imaging findings in the axial and coronal planes (8). This classification does not deal only with the demonstration of the primary fistulous tract, but also with the secondary branching and associated abscesses. Furthermore, this system is simple and satisfactory

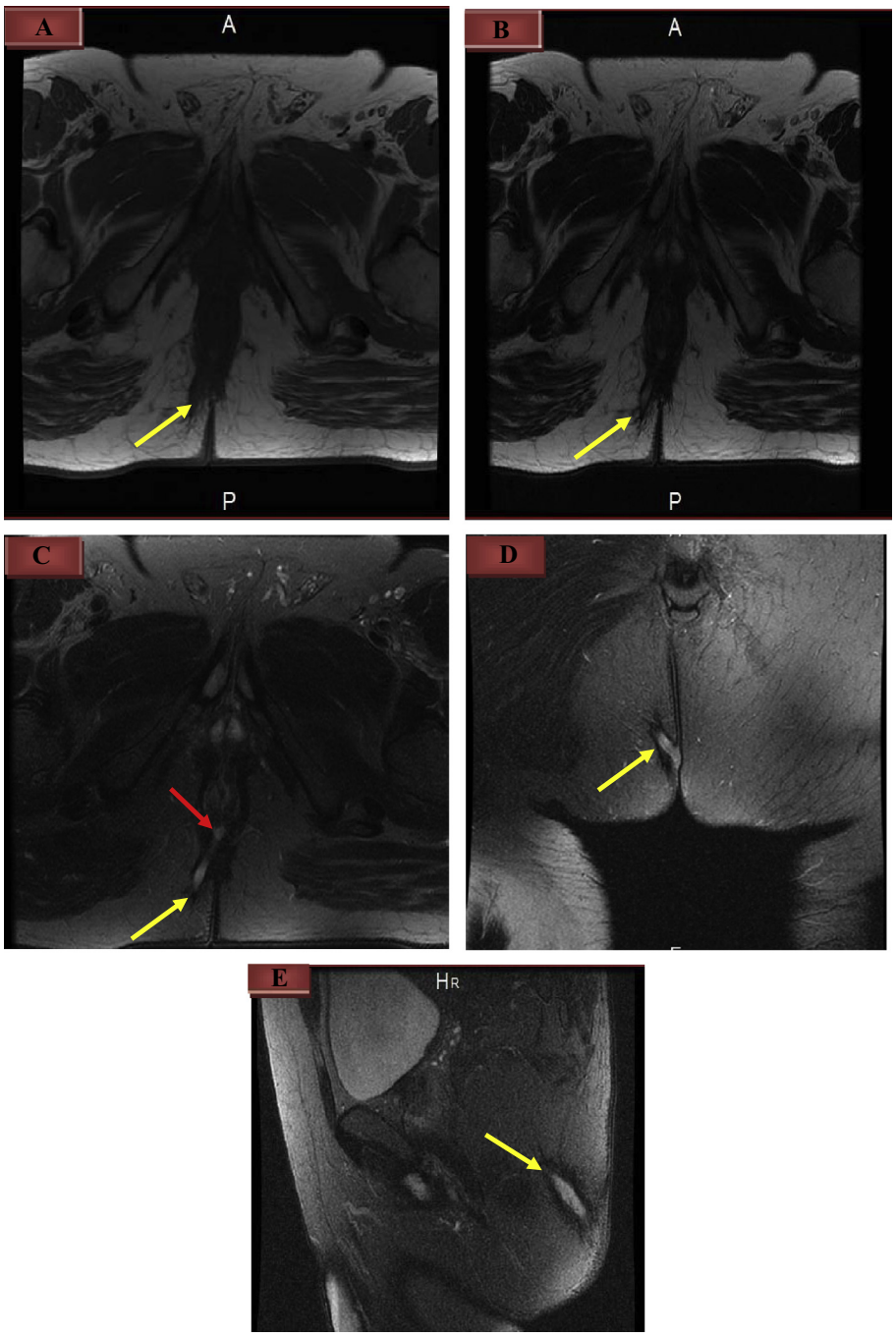

Fig. 6 (A, B, C, D and E) represents a patient with grade 3 right trans-sphincteric non branching fistula with no secondary tract, associated abscess, horseshoe or supralevator extensions. Non-contrast axial T1WFSE (A) and axial T2WFSE (B) as well as axial, coronal and sagittal FS T2WFSE (C, D and E, respectively) images show a right trans-sphincteric non branching fistula with the point of entry of the fistulous tract obviously seen in the midline posteriorly at the 6 o'clock position (red arrow at C image) and the tract itself is seen traversing the external sphincter to the ischio-rectal fossa (yellow arrows at A, B, C and D images).

as it is based on anatomic landmarks in the axial and coronal planes which are well-known to radiologists, with excellent applicability and reproducibility (11).

In the current work, the type of fistula was accurately identified by using the St James's University Hospital classification. The commonest type of ano-rectal fistula was grade 1 (37.5%). This grading successfully correlated with the surgical findings with effective identification of fistulous tracts and associated findings and extensions.

Occasionally, the accurate location of the internal opening can be difficult to recognize due to difficult anatomical conditions as it is usually narrow, small or intermittently closed. Many failures of surgical treatment are correlated to inadequate recognition of the fistula course, or failure in finding

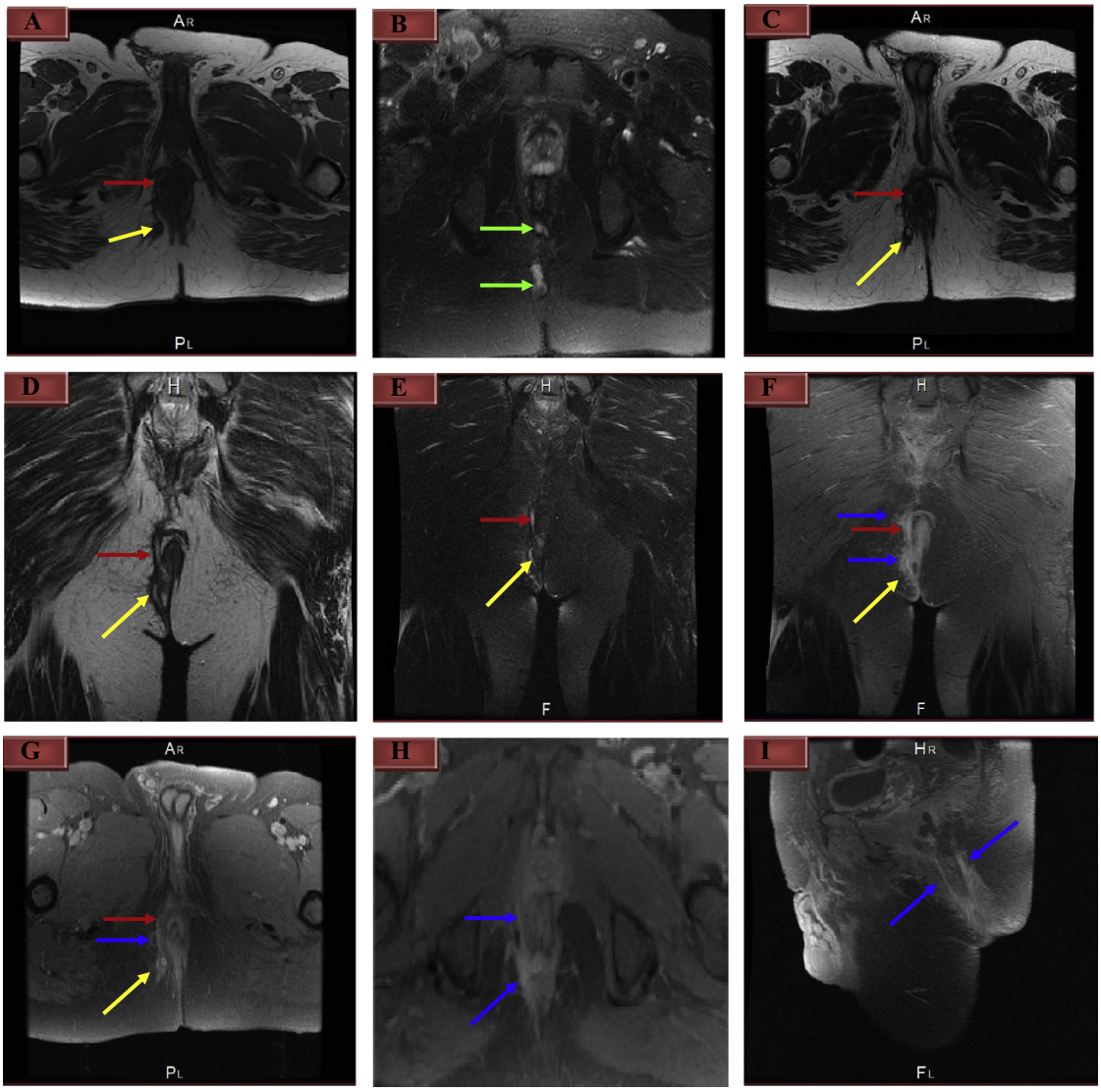

Fig. 7 (A, B, C, D, E, F, G, H and I) represents a patient with grade 4 right branching trans-sphincteric fistula with the secondary track seen within the ischiorectal fossa. Axial T1WFSE (A), axial (C) and coronal (D) T2WFSE, and coronal FS T2WFSE (E) images demonstrate a right sided branching fistulous tract with two branches: the primary, trans-sphincteric branch at a higher level on the right lateral wall of the anal canal near the levator plate (the red arrows at A, C, D and E) and the secondary lower branch is seen in the right inter-sphincteric space (the yellow arrows at A, C, D and E images). Axial plane of FS T2WFSE (B) sequence image demonstrates the site of the internal opening of the two branches of the fistula at 6 o'clock position (the green arrows at B image). Coronal (F), axial (G and H) and sagittal (I) planes of contrast enhanced FS T1WFSE sequence images demonstrate the enhancement of both branches of the fistula with enhancement of the surrounding inflammatory reaction (the blue arrows).

all of the branches or internal orifices (1). Therefore, it is necessary to identify the level and exact site of the internal opening. Most fistulas open into the anal canal at the level of the dentate line and enter posteriorly, around the 6 o'clock position (17).

In this study, the most common location of the internal opening of the ano-rectal fistula was at 6 o'clock position as it was encountered in half of our patients ($n = 12$). The internal openings were accurately identified in all patients via the axial and coronal planes of contrast enhanced FS T1WFSE with accuracy of 100%. On the other hand, the lowest accuracy was encountered on axial and coronal planes of T1WFSE sequence and sagittal plane of T2WFSE sequence (83.3% in each).

The unenhanced T1-weighted images provide an excellent anatomic overview of the sphincter complex, levator plate, and ischio-rectal fossa (8). On gadolinium-enhanced FS T1WFSE images, fistulous tracts and active granulation tissue exhibit intense enhancement, while fluid in the track remains hypointense. Moreover, chronic fistulas with fibrotic tracts appear as linear structures of low signal intensity on T1W and T2W images with no enhancement after administration of contrast material (2,19). The accurate place of the primary tract is most easily seen on axial images as the existence of disruption

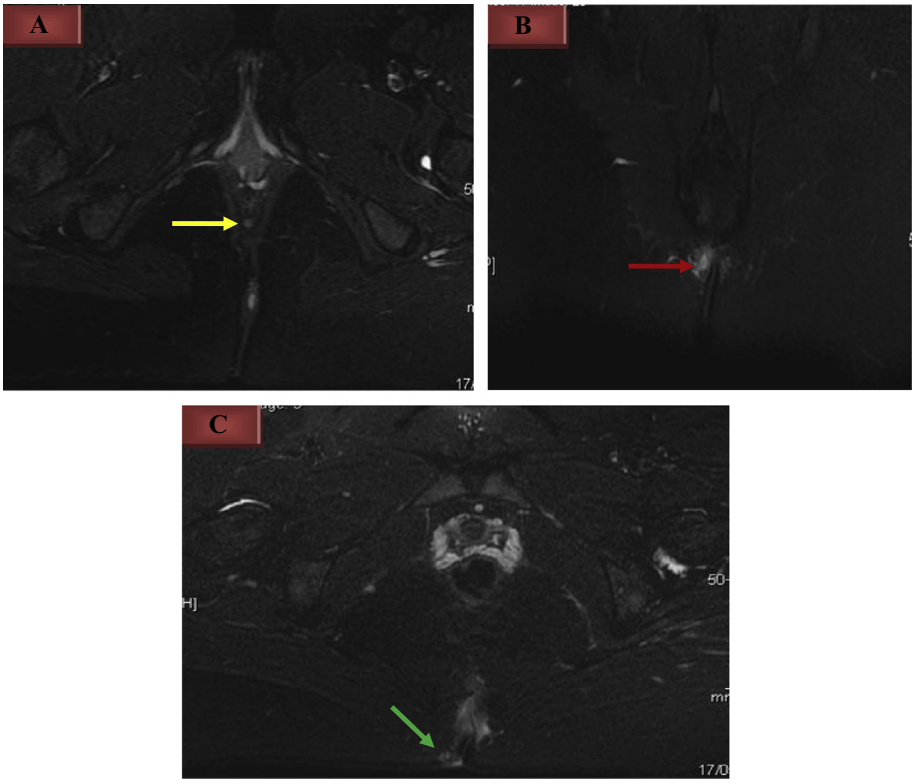

Fig. 8 (A, B and C) represents a patient with grade 4 right trans-sphincteric fistula with an abscess in the right ischioanal fossa. Axial FS T2WFSE (A and B) as well as axial contrast enhanced FS T1WFSE (C) images show a right trans-sphinctric fistula (yellow and red arrows on A and B images, respectively) with enhancement of the inflammatory reactions around the fistulous tract as well as enhancement of the associated abscess cavity which is seen inseparable from the fistulous tract in the right ischioanal fossa (light green arrow on C image). There are no secondary tract, horseshoe or supralevator extensions.

of the external anal sphincter differentiates a trans-sphincteric fistula from an inter-sphincteric one. Coronal images depict the levator plane, thereby allowing differentiation of supra-levator from infra-levator extension (6). Contrast enhanced FS T1WFSE images were found to be as helpful as FS T2WFSE images in identifying the pathology and both are needed to delineate the tracts (20).

The coronal and transverse images are both important in evaluating the course and the anatomical location of the tracts and abscesses. The transverse images are found to be most helpful in recognizing infra-levator tracts and abscesses, while the coronal images were excellent for supra-levator tracts and abscesses in the levator ani muscles (21). Fat suppressed T2-weighted sequences can be used with the T2WFSE to clarify fluid-containing tracts or abscesses, as the high signal intensity of fat can conceal the active fistulous tracts or abscesses, which also have high signal intensity. On FS T2W images; fluid, pus and granulation tissue are seen as areas of high signal intensity on a background of low-signal-intensity fat (2). Additionally, on contrast-enhanced FS T1WFSE images, abscesses demonstrate a central area of low signal intensity due to pus that is surrounded by intense ring enhancement (6,22).

In our work, all simple non branching fistulas were successfully identified by axial and coronal planes of contrast enhanced FS T1WFSE images with an accuracy of 100%, while fistulas with branching tracts were best recognized by using the same sequence but with an accuracy of 95.83%. Additionally, we found that the axial planes of contrast enhanced FS T1WFSE and FS T2WFSE sequences were helpful in recognition of low ano-rectal fistulas (accuracy was 100% and 95.83%, respectively), while the high fistulas were better identified on coronal images of the same sequences with same accuracy. This is going with that reported by many other previous authors (2,6,21). By MRI examination, branching fistula was present in 5 patients (Table 5), but according to surgical data, it was present in 6 patients (Table 6). So, one patient with a faint and high secondary fistulous tract was missed by MRI.

In assessment of ano-rectal abscesses in this study, all the MR sequences had the accuracy of 100% except the sagittal planes of different sequences as well as non-contrast T1WFSE. The inter-sphincteric abscesses are better identified on axial plane of T2WFSE, FS T1WFSE, FS T2WFSE and contrast enhanced FS T1WFSE sequences, while pelvi-rectal abscesses were better recognized on coronal plane of T2WFSE, FS T1WFSE, FS T2WFSE and contrast enhanced FS T1WFSE sequences (accuracy 100% for each sequence).

Supralevator, ischio-anal and horseshoe extensions are common (8). As reported by previous studies (2,6,21), we found that the horseshoe tract extensions and supralevator extensions were better recognized by using the axial and coronal planes of contrast enhanced FS T1WFSE sequence images with accuracy of 100% for each one. In contrary, the accuracy of axial and coronal planes of FS T2WFSE, in identification of horseshoe extensions and supralevator extensions was 95.83%

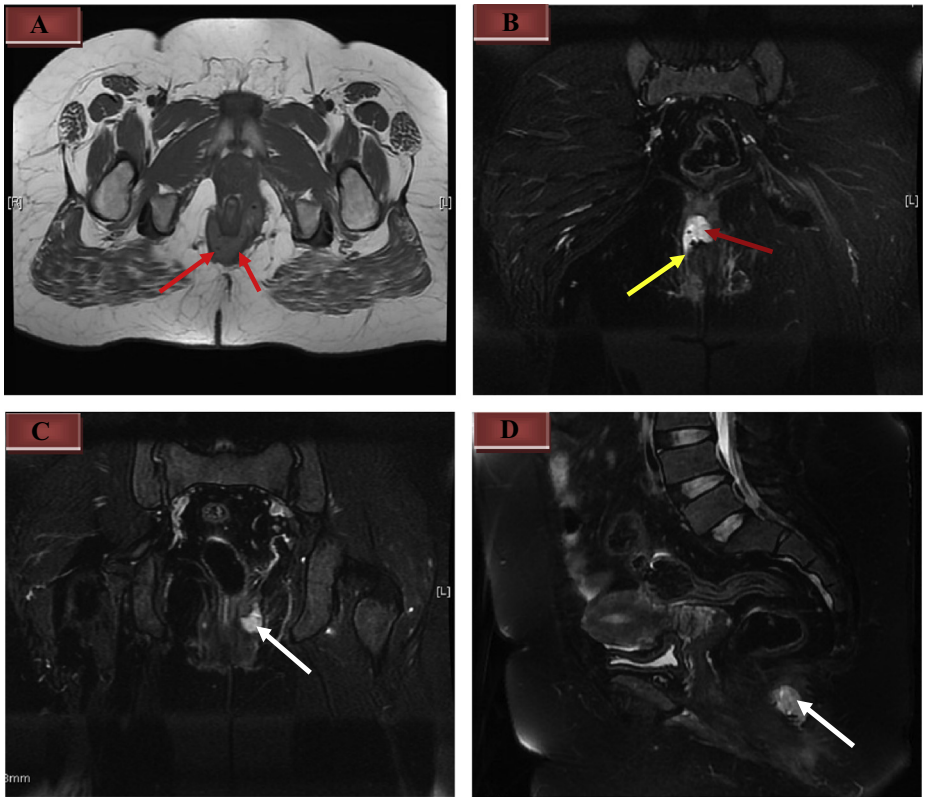

Fig. 9 (A, B, C and D) demonstrates a patient with grade 4 trans-sphincteric fistula associated with branching fistulous tract with an abscess formation in the ischioanal fossa and horseshoe extension in the posterior inter-sphincteric space. Axial T1WFSE (A), coronal contrast enhanced FS T1WFSE (B and C) and sagittal FS T2WFSE (D) sequence images show two fistulous tracts: the primary, trans-sphincteric branch on the left lateral wall of the anal canal, where an associated abscess (white arrows at C and D images) is seen with the signal void appearance of pus as well as a secondary intersphincteric tract at the right side (yellow arrow at B image) with associated horseshoe extension in the posterior intersphincteric space (red arrows at A and B images).

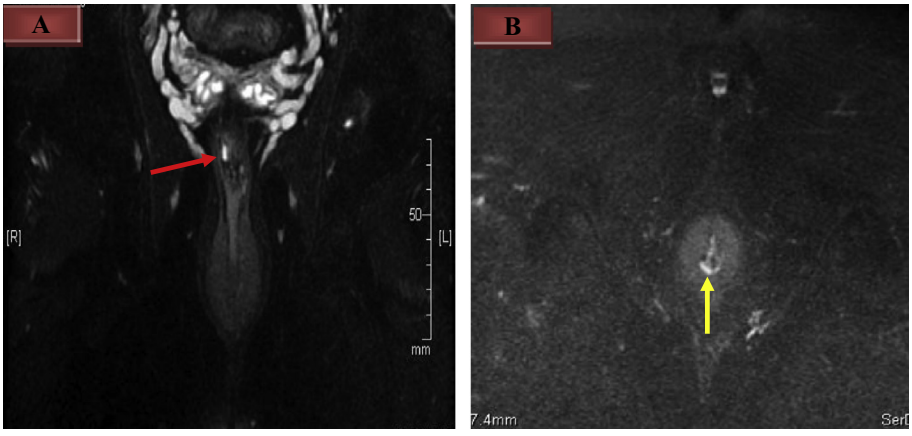

Fig. 10 (A and B) demonstrates a patient with grade 5 right supralevator (supra-sphincteric) fistula. Coronal T2WFSE (A) shows right sided high level supra-sphincteric fistulous tract which arises from the anal canal before ascending to the supralevator space. The axial contrast enhanced FS T1FSE (B) shows the position of the internal opening of the fistula at 6 o'clock. There is no associated secondary tract or abscess formation.

and 100%, respectively. Also, we better recognized the fistula associated inflammatory changes on the coronal and axial planes of contrast enhanced FS T1WFSE sequence images with accuracy of 100%, while the accuracy of sagittal plane of contrast enhanced FS T1WFSE sequence images was 95.8%.

Unfortunately, one of the limitations of our study was the non use of some other MRI sequences to evaluate their

accuracies in diagnosing ano-rectal fistulas; such as three-dimensional T2W turbo spin-echo (3D-T2WTSE), spoiled gradient (SPGR) and maximum intensity projection (MIP) MR imaging due to lack of the software required for such sequences in our machine. Another limitation was the small number of the studied patients. So, studies with a larger number of patients and a broader spectrum of MRI sequences are recommended in future work.

In summary, our results revealed that MRI is an essential useful tool in pre-operative evaluation of the ano-rectal fistula. It provides high resolution images of the anatomy of the ano-rectal region with delicate depiction of the fistulous tracts with their associated secondary ramifications and abscesses. Contrast administration can add more information and assist discrimination between active and inactive tracts with delineation of tracts which are not usually visualized. More specifically, the axial and coronal planes of contrast enhanced FS T1WFSE sequence images represent a significantly high accuracy (99.4%) in identification of ano-rectal fistulas. Moreover, an optimal diagnostic accuracy can be obtained by using a combination of contrast enhanced FS T1WFSE sequence images with either T2WFSE or FS T2WFSE images in both the coronal and axial planes. Such combination is adequate to provide the essential details required for pre-operative evaluation of the ano-rectal fistulas.

Conflict of interest

The authors declared no conflict of interest.

References

(1) Waniczek D, Adamczyk T, Arendt J, Kluczewska E, Kozenska-Marek E. Usefulness assessment of preoperative MRI fistulography in patients with perianal fistulas. Pol J Radiol 2011;76(4):40–4.

(2) George U, Sahota A, Rathore S. MRI in evaluation of perianal fistula. J Med Imag Radiat Oncol 2011;55:391–400.

(3) Morris J, Spencer JA, Ambrose NS. MR imaging classification of perianal fistula and its implications for patient management. Radiographics 2000;20:623–35.

(4) David A, Schwartz DA, Pemberton JH, Sandborn WJ. Diagnosis and treatment of perianal fistulas in Crohn's disease. Ann Intern Med 2001;135(10):906–18.

(5) Bhaya AK, Kumar N. MRI with MR fistulogram for perianal fistula: a successful combination. Clin Gastrointest Magnetom 2007;1:56–9.

(6) Khera PS, Badawi HA, Afifi AH. MRI in perianal fistulae. Indian J Radiol Imag 2010;20(1):53–7.

(7) Yıldırım N, Gökalp G, Öztürk E, Zorluoğlu A, Yilmazlar T, Ercan I, et al. Ideal combination of MRI sequences for perianal fistula classification and the evaluation of additional findings for readers with varying levels of experience. Diagn Interv Radiol 2012;18(1):11–9.

(8) de Miquel Criado J, del Salto LG, Rivas PF, del Hoyo LF, Velasco LG, de las Vacas MI, et al. MR imaging evaluation of perianal fistulas: spectrum of imaging features. RadioGraphics 2012;32:175–94.

(9) Parks AG, Gordon PH, Hardcastle JD. A classification of fistula-in-ano. Br. J. Surg. 1976;63:1–12.

(10) O'Malley RB, Al-Hawary MM, Kaza RK, Wasnik AP, Liu PS, Hussain HK. Rectal imaging: part 2, perianal fistula evaluation on pelvic MRI- what the radiologist needs to know. AJR 2012;199:W43–53.

(11) Lima CO, Junqueira FP, Rodrigues MS. Magnetic resonance imaging evaluation of perianal fistulas: iconographic essay. Radiol Bras 2010;43(5):330–5.

(12) Michalopoulos A, Papadopoulos V, Tziris N, Apostolidis S. Perianal fistulas. Tech Coloproctol 2010;14(1):S15–7.

(13) Laniado M, Makowiec F, Dammann F, Jehle EC, Claussen CD, Starlinger M. Perianal complications of Crohn's disease: MR imaging findings. Eur Radiol 1997;7:1035–42.

(14) Holschneider A, Hutson J, Pena A, Beket E, Chatterjee S, Coran A, et al. Preliminary report on the international conference for the development of standards for the treatment of ano-rectal malformations. J Pediatr Surg 2005;40:1521–6.

(15) Oliver S, Christian L, Mathias L. Assessment of anal fistulas with high resolution subtraction MR fistulography: comparison with surgical findings. J Magn Reson Imaging 2004;19(1):91–8.

(16) Kubota A, Kawahara H, Okuyama H, Oue T, Tazuke Y, Tanaka N, et al. Laparoscopically assisted anorectoplasty using perineal ultrasonographic guide. J Pediatr Surg 2005;40:1535–8.

(17) Halligan S, Stoker J. Imaging of fistula in ano. Radiology 2006;239:18–33.

(18) Holzer B, Rosen HR, Urban M, Anzböck W, Schiessel R, Hruby W. Magnetic resonance imaging of perianal fistulas: predictive value for Parks classification and identification of the internal opening. Colorectal Dis J 2000;2(6):340–5.

(19) Beets-Tan RG, Beets GL, van der Hoop AG, Kessels AG, Vliegen RF, Baeten CG, et al. Preoperative MR imaging of anal fistulas: does it really help the surgeon? Radiology 2001;218(1):75–84.

(20) Torkzad MR, Karlbom U. MRI for assessment of anal fistula. Insights Imaging 2010;1:62–71.

(21) Al-Khawaria HA, Guptaa R, Sinana TS, Prakashb B, Al-Amerb A, Al-Bolushic S. Role of magnetic resonance imaging in the assessment of perianal fistulas. Med Princ Pract 2005;14:46–52.

(22) Spencer JA, Ward J, Beckingham IJ, Adams C, Ambrose NS. Dynamic contrast-enhanced MR imaging of perianal fistulas. AJR Am J Roentgenol 1996;167(3):735–41.